AGE (2010) 32:161–177
DOI 10.1007/s11357-009-9121-4

Both endoplasmic reticulum and mitochondria are involved in disc cell apoptosis and intervertebral disc degeneration in rats

Chang-Qing Zhao · Yue-Hui Zhang · Sheng-Dan Jiang · Lei-Sheng Jiang · Li-Yang Dai

Received: 22 July 2009 / Accepted: 10 November 2009 / Published online: 4 December 2009

Abstract Intervertebral disc cell apoptosis occurs through either death receptor or mitochondrial pathway, but whether disc cell apoptosis is also mediated by the endoplasmic reticulum (ER) pathway remains unclear. The objective of this study was to investigate whether ER and mitochondria are co-involved in disc cell apoptosis and intervertebral disc degeneration (IVDD) in rats. Forty-eight rats were used for in vivo experiments. IVDD was characterized by X-ray and histomorphology examination, disc cell apoptosis was detected by TUNEL staining, and the co-involvement of ER and mitochondria in apoptosis was determined by immunohistochemical staining for GRP78, GADD153, caspase-12, and cytochrome C. Additional eight rats were used for annular cell isolation and culture. After sodium nitroprusside treatment, annular cell apoptosis was observed morphologically and quantified by flow cytometry; the expression of biomarkers of ER stress and mitochondrial dysfunction were analyzed by reverse transcriptase PCR (RT-PCR), fluorescence double labeling, and Western blot; and mitochondrial membrane potential was detected by 5′,6,6′-tetrachloro-1,1′,3,3′-tetraethylbenzimidazolcarbo cyanine iodide (JC-1) staining. Finally, NS3694 and Z-ATAD-FMK were employed to inhibit the formation of apoptosome complex and the activation of caspase-12, respectively, and apoptotic incidence and caspase-9 activity were assayed. We found that IVDD, induced by unbalanced dynamic and static forces in the rats, was accompanied by increased disc cell apoptosis and enhanced expression of GRP78, GADD153, caspase-12, and cytochrome C. Annular cell apoptosis induced by sodium nitroprusside was confirmed by morphologic observation and flow cytometry. With increased apoptosis, the expression of GRP78, GADD153, and caspase-12 upregulated, mitochondrial membrane potential decreased, and accumulation of cytochrome C in the cytosol manifested. Furthermore, NS3694 and Z-ATAD-FMK dramatically suppress annular cell apoptosis and caspase-9 activity. In conclusion, disc cell apoptosis mediated simultaneously by ER and mitochondria plays a potent role in IVDD.

Keywords Intervertebral disc degeneration · Apoptosis · Endplasmic reticulum · Mitochondria

C.-Q. Zhao and Y.-H. Zhang contributed equally to this paper.

C.-Q. Zhao · Y.-H. Zhang · S.-D. Jiang · L.-S. Jiang · L.-Y. Dai
Department of Orthopedic Surgery, Xinhua Hospital, Shanghai Jiaotong University School of Medicine, Shanghai, China

L.-Y. Dai (✉)
Department of Orthopedic Surgery, Xinhua Hospital, 1665 Kongjiang Road, 200092 Shanghai, China
e-mail: chinaspine@163.com

Introduction

Tissue destruction and altered function of the intervertebral discs, commonly referred to as intervertebral disc degeneration (IVDD), is the primary cause of back pain, secondary spinal deformity, and neural compressive disorders, which impose a huge burden on the health care system around the world. Among many genetic and environmental factors that may contribute to the development of IVDD, disc cell death through apoptosis appears to be a major component (Ariga et al. 2001, 2003; Court et al. 2001; Gruber and Hanley 1998; Kohyama et al. 2000; Kroeber et al. 2002; Lotz and Chin 2000; Lotz et al. 1998; Park et al. 2001a,b, 2005, 2006; Rannou et al. 2004; Walsh and Lotz 2004; Wang et al. 2006a; Zhao et al. 2006, 2007), but the signal transduction pathways involved in disc cell apoptosis have not been fully understood.

Previous studies have shown that disc cell apoptosis occurs through either death receptor (Park et al. 2001a, b, 2006) or mitochondrial (Rannou et al. 2004) pathway, as confirmed by the activation of caspase-8 or caspase-9, and that the cross-talk between these two pathways also mediates disc cell apoptosis (Park et al. 2005). However, specific inhibitors of caspase-8 or caspase-9 can only partially suppress apoptosis of cultured disc cells (Park et al. 2005; Rannou et al. 2004), suggesting that disc cell apoptosis may be also mediated by other signal transduction pathways, for instance, the endoplasmic reticulum (ER) pathway.

The ER, the organelle for synthesis of numerous proteins and formation of their proper tertiary structure, also acts as a dynamic Ca^{2+} reservoir responsible for fast physiological signal transduction. Various intracellular and extracellular stimuli can affect the functions of the ER, leading to the so-called ER stress. Generally, ER stress is referred to a series of molecular and biochemical alternations inside the cells due to ER dyshomeostasis, mainly including dysfunction of protein folding, impairment of protein transportation, and depletion of Ca^{2+} in the ER lumen (Kadowaki et al. 2004; Groenendyk and Michalak 2005). The unfolded and misfolded proteins activate a self-protective mechanism to upregulate the expression of some ER resident chaperones, such as glucose regulated protein 78 (GRP78), giving the affected cells a chance to survive (Reddy et al. 2003; Luo et al. 2006). When the cells are exposed to prolonged or strong ER stress, however, the expression of some apoptosis promoters, such as growth arrest and DNA damage-inducible gene 153 (GADD153), increases (Benavides et al. 2005; McCullough et al. 2001), caspase-12 is activated and in turn activates caspase-9 and caspase-3 (Morishima et al. 2002; Tan et al. 2006), resulting in apoptotic cell death. Because ER stress is so crucial to cell survival or death, it has become an attractive research focus in recent years. In fact, there is a great body of evidence indicating that apoptosis mediated by ER plays an important role in degenerative diseases such as Alzheimer's disease (Unterberger et al. 2006; Williams and Lipkin 2006), amyotrophic lateral sclerosis (Nagata et al. 2007), senile cataract (Mulhern et al. 2006), and osteoarthritis (Oliver et al. 2005; Yang et al. 2005).

Furthermore, apoptosis is a very complex process which includes many signal transduction pathways and the delicate interactions among them. As pointed out by Adams (2003) in their review, apoptosis can be simultaneously mediated by two or more signal pathways, but their relative importance is different in response to specific stimuli. For instance, many cell types such as astrocytes (Liu et al. 2004), mouse embryonic fibroblasts (Masud et al. 2007; Sanges and Marigo 2006), Hela cells (Xu et al. 2006), and human teratoma cells (Ferreiro et al. 2008) undergo apoptosis through both mitochondrial and ER pathway, and there is evidence showing that both death receptor and mitochondrial pathway simultaneously contribute to disc cell apoptosis (Park et al. 2005). We thus hypothesize that mitochondria and the ER might also be co-involved in disc cell apoptosis and therefore play a role in IVDD.

Here, we show that disc cell apoptosis occurred through both mitochondrial and ER pathway in degenerated rat lumbar discs induced by unbalanced dynamic and static forces. The co-involvement of mitochondrial and ER pathway in disc cell apoptosis was further tested in vitro by treating rat annular cells maintained in a monolayer with sodium nitroprusside (nitric oxide donor), a potent in vitro reactive oxygen species commonly used to induce apoptosis in many cell types.

Materials and methods

Experimental studies were approved by the authors' institutional Animal Care and Use Committee.

In vivo experiments

Rat model of lumbar IVDD

A total of 48 male Sprague–Dawley rats, aged 2 months, were used for the in vivo experiments. The rats were randomly divided into six groups, with eight rats in each group. To develop lumbar IVDD, rats in three of six groups received a surgical procedure, which is a modified version established by Wang et al. (2006a) and leads to unbalanced dynamic and static forces of the lumbar spine. Briefly, through a dorsal medial approach under general anesthesia, the sacrospinal muscles, spinous processes, supraspinous ligaments, interspinous ligaments, posterolateral 1/2 of bilateral zygapophysial joints of the lumbar spine were removed. Rats in the other three groups received a skin incision and saturation and severed as controls.

X-ray examination of IVDD

At the 6-, 12-, and 18-week points after surgery, rats in one model group and one control group were used for X-ray examination, respectively. Under general anesthesia, lateral radiophotographs of the lumbar spine of each rat were obtained by use of a Toshiba KXO-32R X-ray machine. IVDD was evaluated in terms of disc space narrowing, endplate calcification and malalignment of the lumbar spine.

Histomorphology evaluation of the lumbar spine

After X-ray examination, the rats were euthanized by intraperitoneal administration of overdose pentobarbital sodium. Lumbar spines including L4 to L6 levels were taken out en bloc; the paravertebral muscles and the posterior columns were removed thoroughly. The specimens were then fixed in 4% paraformaldehyde for 48 h, decalcified at 4°C in 20% ethylenediamine tetraacetic acid for 5–7 weeks, embedded in paraffin, and sectioned (4 μm) along the midsagittal plane. Sections were used for hematoxylin–eosin (HE), terminal deoxynucleotidyl transferase [TdT]-mediated dUTP nick end labeling (TUNEL) or immunohistochemistical staining.

IVDD was scored based on histomorphologic features of HE-stained sections according to the classification system established by Nishimura and Mochida (1998). The average score of L4-5 and L5-6 was recorded as the grade of lumbar IVDD in each rat.

Apoptosis detection by TUNEL staining

In situ TUNEL reaction was performed on two serial sections per specimen (including four discs in total) using MK1020 Apoptosis Detection Kit (Boster) according to the manufacturer's instructions; sections treated without TdT served as negative controls. Total and TUNEL-positive disc cells were counted below three to five noncontinuous high-power fields (magnification, ×400) in each of three regions (cartilaginous endplate, annulus fibrosus, and nucleus pulposus) from each of four discs per specimen and summed up. The percentage of TUNEL-positive disc cells compared with total disc cells was then calculated.

Immunohistochemistry studies for GRP78, GADD153, caspase-12, and cytochrome C

Immunohistochemistry for GRP78, GADD153, caspase-12, and cytochrome C was performed on paraffin-embedded sections using the streptavidin–biotin peroxidase complex method. After antigen retrieval, quenching of endogenous peroxidase, and blocking of nonspecific binding, sections were incubated with rabbit polyclonal antibody against GRP78 (Santa Cruz, sc-13968; 1:75 dilution), mouse monoclonal antibody against GADD153 (Santa Cruz, sc-7351; 1:75 dilution), rabbit polyclonal antibody against caspase-12 (Santa Cruz, sc-5627; 1:75 dilution), or rabbit polyclonal antibody against cytochrome C (Santa Cruz, sc-7159; 1:75 dilution) [as shown by Rannou et al. (2004), this antibody cannot penetrate the mitochondrial membrane, thus only detecting cytochrome C released from the mitochondria] at 4°C overnight. Following sequential treatment with biotinylated goat anti-rabbit or anti-mouse immunoglobulin (IgG) and streptavidin–biotin horseradish peroxidase complex, the sections were colorized with 3,3-diaminobenzidine tetrahydrochloride and hydrogen peroxide and counterstained with hematoxylin. Sections in which the primary antibodies were omitted were used as negative controls. The percentage of GRP78-, GADD153-, caspase-12-, and cytochrome C-positive disc cells was

calculated as TUNEL-positive disc cells, as described above.

In vitro experiments

A diagram (Fig. 1) shows our design of in vitro experiments.

Isolation and culture of rat annular cells

Eight male Sprague–Dawley rats, aged 3 months, were used for the in vitro experiments. Our established method for isolation and primary culture of rat annular cells (Zhao et al. 2007) was employed, and first-passage cells maintained in a monolayer were used throughout the in vitro experiments.

Identification of apoptotic cells by morphology

Primary cells were subcultured in six-well plates at 2×10^5 cells per well with Dulbecco's modified Eagle medium/Ham's F-12 (DMEM/F-12) containing 10% fetal bovine serum and antibiotics. After reaching 80–90% confluence, the medium was changed, and sodium nitroprusside was added to the medium to a final concentration of 0.5 mM. At the 0-, 1-, 2-, 4-, and 6-h points after the addition of sodium nitroprusside, dynamic morphologic changes of rat annular cells in the selected region in the well was consecutively observed using an inverted phase-contrast microscopy. As described by Fernandez-Segura et al. (1999), apoptotic cells exhibited shrinkage and plasma membrane blebbing.

Apoptosis detection by flow cytometry

Primary cells were seeded into five wells of six-well plates at 2×10^5 cells per well and treated similarly. At the 0-, 1-, 2-, 4-, and 6-h points after treatment with 0.5 mM sodium nitroprusside, apoptotic incidence of rat annular cells was detected using the Annexin V-FITC apoptosis detection kit I (BD

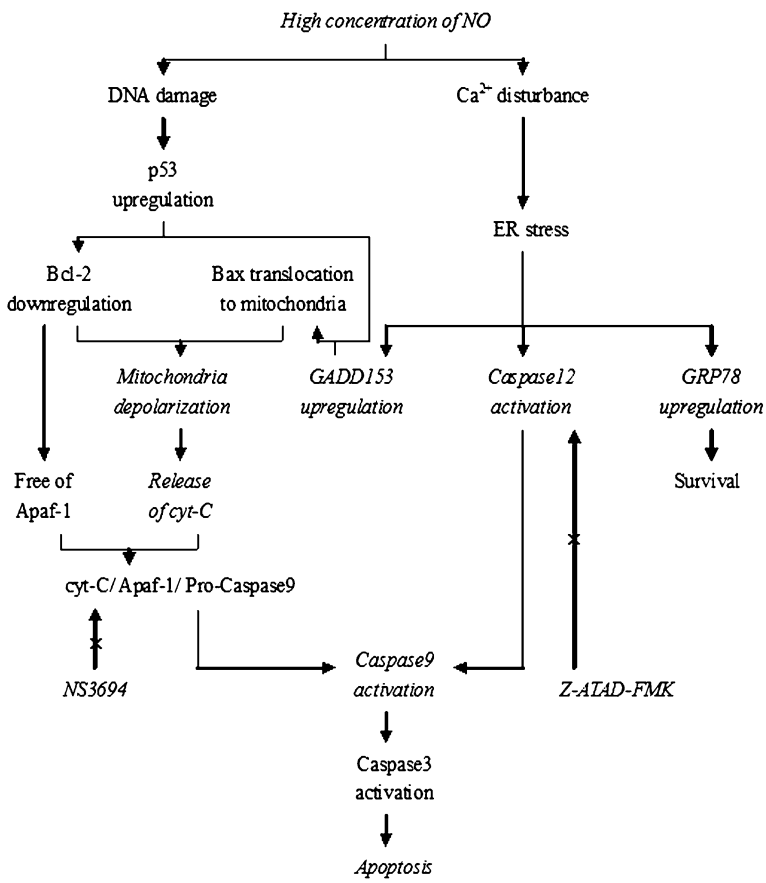

Fig. 1 Cross-talk between mitochondria and ER in NO-induced apoptosis. Contents shown in *italic type* within the diagram were studied

Pharmingen), as described previously (Zhao et al. 2007).

Reverse transcriptase PCR

Primary cells were seeded into six-well plates and treated as described above. At the 0-, 1-, 2-, 4-, and 6-h points after treatment with 0.5 mM sodium nitroprusside, cells were harvested, and total RNA was extracted using Trizol reagent (Invitrogen) following the manufacturer's instructions. A total of 750 ng of RNA was reverse-transcribed into complementary DNA using a Reverse Transcription Kit (TaKaRa, DRR037S). Primers for GRP78, GADD153, caspase-12, and β-actin were designed with Primer Premier 5.0 and Oligo 6 software programs and obtained from Shanghai Sangon Biological Engineering Technology & Services Co., Ltd (China). The upstream and downstream primer sequences for each gene of interest were as follows: GRP78, 5′-ACT GGA ATC CCT CCT GCT C-3′ and 5′- CAA ACT TCT CGG CGT CAT-3′; GADD153, 5′-GCC TTT CGC CTT TGA GAC-3′ and 5′-CTT TGG GAG GTG CTT GTG-3′; caspase-12, 5′- AGT CCT CCG ACA GCA CAT-3′ and 5′-AGT TCA CCT GG GAC CTC A-3′; and β-actin, 5′- CCG TAA AGA CCT CTA TGC CAA CA-3′ and 5′-CGG ACT CAT CGT ACT CCT GCT-3′. PCR amplification was performed using the Ex Taq® Kit (TaKaRa, DRR001A). Electrophoresis of the PCR products was performed on 1.5% agarose gel and stained with ethidium bromide. Under ultraviolet irradiation, photographs of the gels were taken and analyzed using SmartView 5.08.057 software program. Band intensity was determined densitometrically and represented as folds of the constitutively expressed gene β-actin.

Fluorescence double labeling study

Primary cells were seeded onto sterile glass coverslips placed in 24-well plates at 5×10^4 cells per well. When reaching 60–70% confluence, the medium was changed, and sodium nitroprusside was added to the medium to a final concentration of 0.5 mM. At the 0-, 3-, and 6-h points after the addition of sodium nitroprusside, the coverslips were harvested, fixed in 4% paraformaldehyde for 15 min, and penetrated in 0.1% Triton for 10 min. After blocking of nonspecific binding, the coverslips were incubated overnight at 4°C with mouse monoclonal antibody against GADD153 (Santa Cruz, sc-7351; 1:75 dilution) and rabbit polyclonal antibody against GRP78 (Santa Cruz, sc-13968; 1:75 dilution), or with mouse monoclonal antibody against GADD153 (Santa Cruz, sc-7351; 1:75 dilution) and rabbit polyclonal antibody against caspase-12 (Santa Cruz, sc-5627; 1:75 dilution), followed by incubation in the dark with mixture of goat anti-mouse IgG linked with Cy3 (1:100 dilution) and goat anti-rabbit IgG linked with fluorescein isothiocyanate (1:100 dilution) for 20 min. The nucleus was counterstained with 2 μg/ml Hoechst 33258 (Sigma) for 5 min, and the coverslips were mounted onto slides using antifade mounting medium (Beyotime). Under the same field, morphologic changes in apoptotic nuclei and the expressions of GRP78, GADD153, and caspase-12 were observed using a fluorescence microscope (Olympus IX50), with Hoechst 33258 excited by ultraviolet light, Cy3 by green light, and fluorescein isothiocyanate by blue light.

Western blot

Primary cells were seeded into 6-cm wells at 6×10^5 cells per well. After reaching 60–70% confluence, the medium was changed, sodium nitroprusside was added to the medium to a final concentration of 0.5 mM. Cells were harvested, and total protein was extracted using a Western & IP Cell Lysis Kit (Beyotime) at the 0-, 1-, 2-, 4-, and 6-h points after sodium nitroprusside treatment, or cytoplasmic protein was extracted using a Mitochondrial Isolation Kit (Applygen) at the 0-, 3-, and 6-h points after sodium nitroprusside treatment. The protein concentrations were measured using a Bradford Protein Assay Kit (Beyotime). Lysates equivalent to 40 μg of protein from each sample were electrophoresed on 10% sodium dodecyl sulfate polyacrylamide gel and transferred to nitrocellulose membranes. After blocking of nonspecific binding with nonfat milk, the membranes were incubated with rabbit polyclonal antibody against GRP78 (Santa Cruz, sc-13968; 1:100 dilution), rabbit polyclonal antibody against caspase-12 (Santa Cruz, sc-5627; 1:75 dilution), mouse monoclonal antibody against cytochrome C (Santa Cruz, sc-13561; 1:100 dilution), and mouse monoclonal antibody against β-actin (Beyotime, AA128; 1:750 dilution) and labeled with horseradish

peroxidase-conjugated secondary antibodies. The immunoreactive bands were visualized by the Super Signal Chemilumnescent Substrate system (Pierce). The images of Western blot study were quantified by plotting a two-dimensional densitogram with SmartView 5.08.057 software program, and band intensity of GRP78, caspase-12, and cytochrome C was expressed as folds of that of β-actin.

Evaluation of mitochondrial membrane potential by flow cytometry

Cells were manipulated as described in "Apoptosis detection by flow cytometry," and mitochondrial membrane potential was determined using a Mitochondrial Membrane Potential Assay Kit with JC-1 (Applygen) following the manufacturer's instructions. Briefly, the harvested cells were resuspended in the mixture of 0.5 ml culture medium and 0.5 ml (JC-1) staining fluid and incubated at 37°C in the dark for 20 min. After washed with cold staining buffer two times, cells were resuspended in 0.5 ml cold staining buffer and analyzed by flow cytometry. The values of mitochondrial membrane potential from each sample were expressed as ratios of red fluorescence intensity over green fluorescence intensity.

Observation of mitochondrial membrane potential in situ

Primary cells were seeded into 3.5-cm wells at 2×10^5 cells per well and treated with 0.5 mM sodium nitroprusside when reaching 60–70% confluence. At the 0-, 3-, and 6-h points after sodium nitroprusside treatment, cells were incubated with the mixture of 1 ml culture medium and 1 ml JC-1 staining fluid at 37°C in the dark for 20 min. After washed with cold staining buffer two times, 2 ml culture medium was added to the well and the excited red light of JC-1 polymer was observed under a fluorescence microscope.

Suppression of apoptosis by NS3694 and Z-ATAD-FMK

Primary cells were seeded into six-well plates at 2×10^5 cells per well. After reaching 80–90% confluence, the medium was changed, and cells in each well were treated as follows: the first well was severed as negative control; the second well was severed as positive control by adding thapsigargin (Alexis) to a final concentration of 1 μM; the third well was added with sodium nitroprusside to a final concentration of 0.5 mM; the fourth, fifth, and sixth wells were pre-incubated with 100 μM NS3694 [a diarylurea compound, which specifically suppresses the cytochrome C-induced formation of apoptosome complex and caspase-9 activation, thus inhibiting the mitochondria-mediated apoptosis (Lademann et al. 2003); Calbiochem®], 2 μM Z-ATAD-FMK [a specific inhibitor of caspase-12, thus suppressing the ER-mediated apoptosis (Luthra et al. 2008); BioVision], and both for 1 h, respectively, followed by treated with 0.5 mM sodium nitroprusside. After 6-h treatment, cells were harvested for the detection of apoptotic incidence as described above.

Caspase-9 activity assay

Cells were cultured and treated as described in "Suppression of apoptosis by NS3694 and Z-ATAD-FMK" with the omission of positive control. At the end of treatment, cells were harvested, and caspase-9 activity was assayed with a Caspase-9 activity kit (Beyotime) following the manufacturer's instructions. Caspase-9 activities from each sample were quantified with a microplate spectrophotometer (Biotek) at an absorbance of 405 nm and expressed as the folds of enzyme activity compared to that of the negative control.

Statistical analysis

Statistical analyses were performed using the SPSS 11.5 statistical software program. According to the data distribution and the homogeneity of variance, one-way ANOVA, Kruskal–Wallis H test, unpaired t test, or Mann–Whitney U test was selectively employed for data comparison between groups, and Pearson correlation test or Spearman rank correlation test was used for correlation analysis. A $P<0.05$ was considered statistically significant.

Results

Characterization of rat lumbar IVDD induced by unbalanced dynamic and static forces

To study the molecular mechanism of IVDD, we first characterized a rat model of IVDD induced by

unbalanced dynamic and static forces of lumbar spine. Conventional X-ray examination revealed normal alignment of lumbar spine without disc space narrowing and endplate calcification in control group rats. In contrast, unbalanced dynamic and static forces induced progressive degenerative changes over time, including lumbar spine malalignment, disc space narrowing and endplate calcification (Fig. 2a). Degeneration of the lumbar intervertebral discs induced by unbalanced dynamic and static forces was also confirmed by histomorphology evaluations. As shown in Fig. 2b and c, the annulus fibrosus of discs in control groups showed normal structure or mildly serpentine appearance, whereas those of the surgical groups manifested mild to moderate and eventually severe serpentine appearance with reversed contour, rupture, or indistinct at the 6-, 12-, and 18-week points after procedure, respectively.

Disc cell apoptosis via both mitochondrial and ER pathway in situ

In control group specimens, very few apoptotic cells were observed under the microscope. In surgical group discs, there was a significant increase in apoptosis in the nucleus pulposus and inner annulus fibrosus as early as 6 weeks after the procedure. When examined 12- and 18-weeks postsurgery, the number of apoptotic cells in the discs remained increased, with the apoptotic cells extending further into outer annulus fibrosus and cartilaginous endplate (Fig. 3a, b). To investigate the potential involvement of ER stress and mitochondrial dysfunction in rat disc cell apoptosis induced by unbalanced dynamic and static forces, we next examined the expression of GRP78, GADD153, caspase-12, and cytochrome C, hallmarks of ER and mitochondria involvement at the protein level. At the 6-, 12-, and 18-week points after

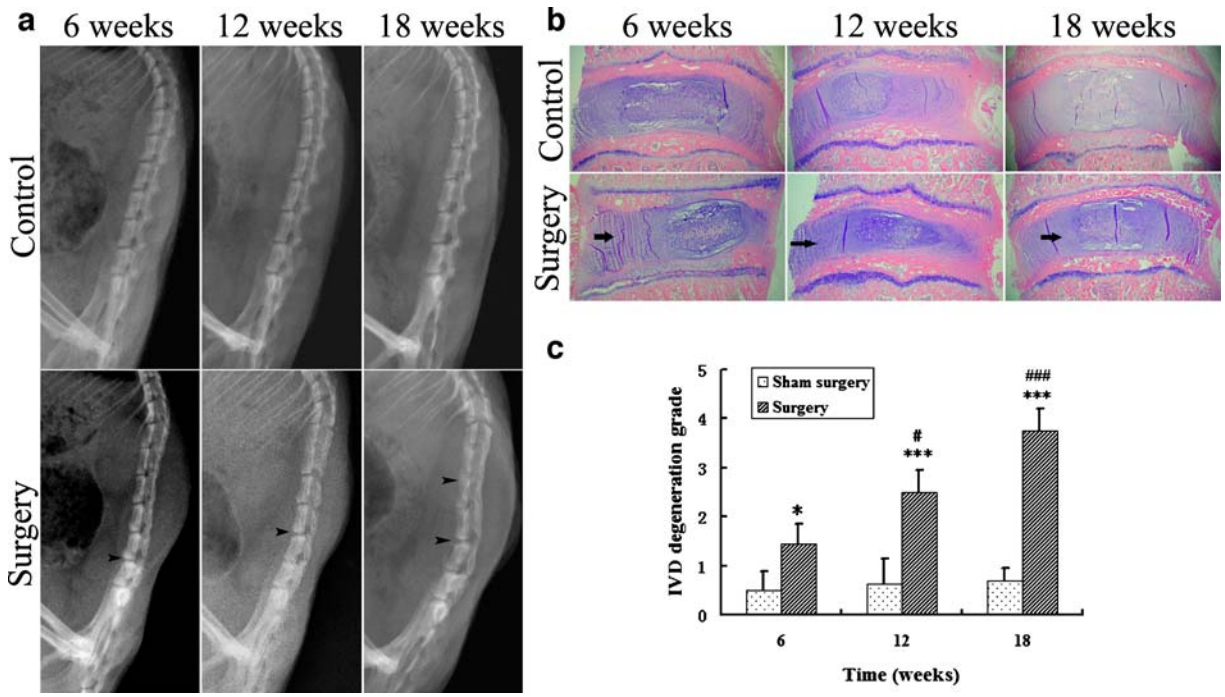

Fig. 2 Characterization of rat lumbar IVDD induced by unbalanced dynamic and static forces. **a** Lateral radiophotographies of the rat lumbar spine. Sham surgery did not cause lumbar spine degeneration; unbalanced dynamic and static forces of lumbar spine led to malalignment, disc space narrowing, and endplate calcification (*arrow heads*). **b** HE staining (original magnification, ×30). The control group annulus fibrosus showed normal structure or mildly serpentine appearance, but the surgical group annulus fibrosus showed moderately to severely serpentine appearance with rupture, reversed contour, or indistinct (*arrows*). **c** Comparison of the grade of IVDD between groups. Comparison between the control group and the surgical group at each time point, $^{*}P<0.05$, $^{***}P<0.001$. In surgical groups, the 12- and 18-week point were compared with the 6-week point, $^{\#}P<0.05$, $^{\#\#\#}P<0.001$

sham surgery, there were a small number of GRP78- and GADD153-positive cells in control group specimens, whereas few caspase-12- and cytochrome C-positive cells were observed. Unbalance of lumbar spine significantly upregulated the expression of GRP78, GADD153, caspase-12, and cytochrome C by disc cells in a time-dependent manner (Fig. 3c–g). In addition, the Spearman rank correlation test also revealed a significant positive relationship between the grade of IVDD and apoptotic incidence (r=0.889, P<0.001). Furthermore, the degree of disc cell apoptosis was also significantly correlated to the expression of GRP78 (r=0.905, P<0.001), GADD153 (r=0.888, P<0.001), and caspase-12 (r=0.798, P<0.001), as well as the amount of cytochrome C released from the mitochondria (r=0.964, P<0.001).

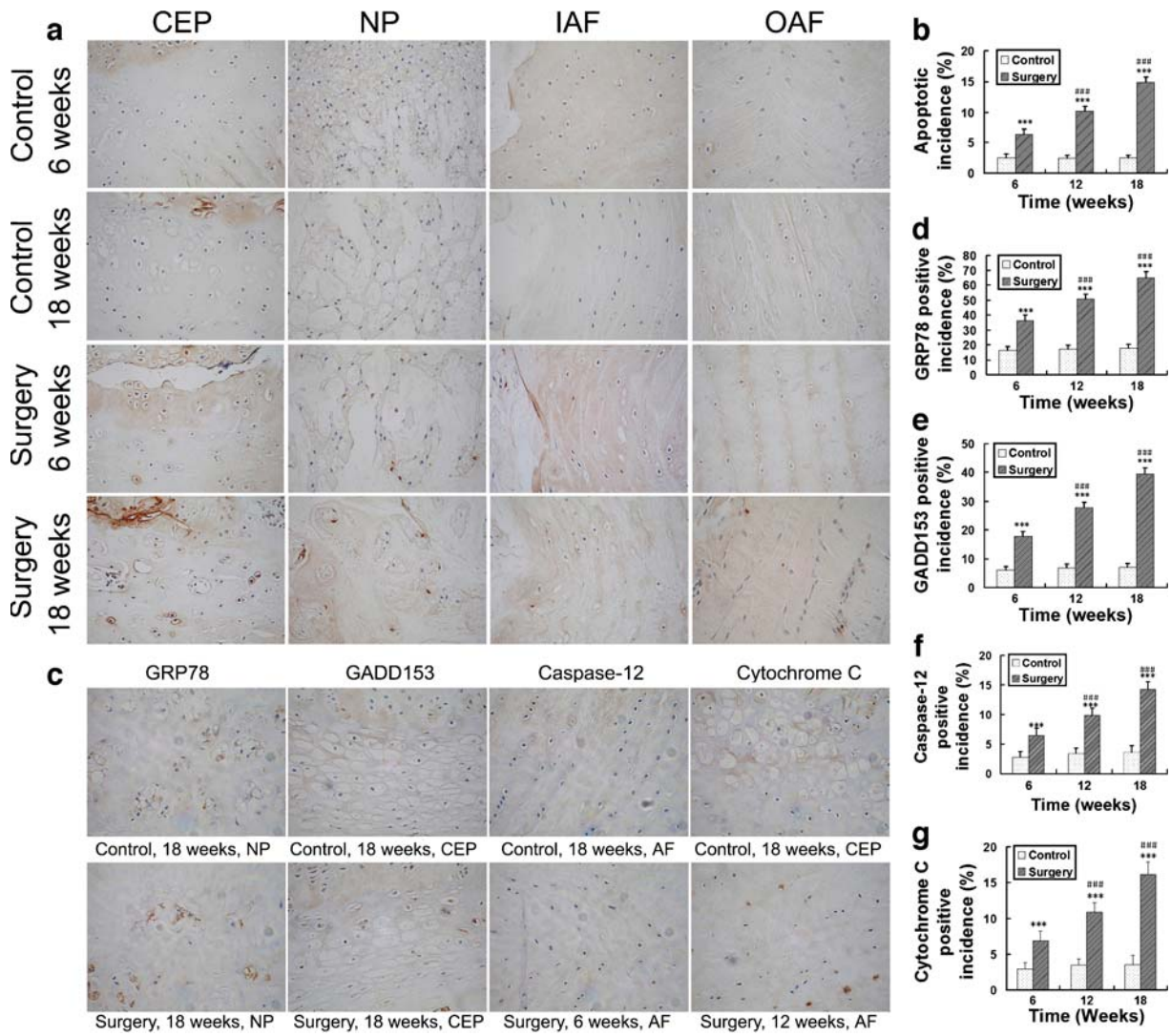

Fig. 3 Disc cell apoptosis via both mitochondrial and ER pathway in situ. **a** TUNEL staining (original magnification, ×320). *CEP* cartilaginous endplate, *IAF* inner annulus fibrosus, *OAF* outer annulus fibrosus, *NP* nucleus pulposus. **b** Comparison of apoptotic incidence between groups. Comparison between the control group and the surgical group at each time point, ***P<0.001. In surgical groups, the 12- and 18-week points were compared with the 6-week point, $^{\#\#\#}P$<0.001. **c** Immunohistochemical stain for GRP78, GADD153, caspase-12, and cytochrome C (original magnification, ×320). **d**–**g** Comparison of the percentage of GRP78-, GADD153-, caspase-12- and cytochrome C-positive cells between groups. Comparison between the control group and the surgical group at each time point, ***P<0.001. In surgical groups, the 12- and 18-week points were compared with the 6-week point, $^{\#\#\#}P$<0.001

Sodium nitroprusside-induced rat annular cell apoptosis detected by morphology and flow cytometry

We visualized apoptotic cells under an inverted phase-contrast microscopy. Following the exposure to 0.5 mM sodium nitroprusside, the initially spread-shaped annular cells maintained in a monolayer sequentially displayed shrink in size, plasma membrane blebbing, shedding of smaller fragments from the cells, and detaching of the whole cell from the culture dish, confirming that the cell death occurred in an apoptotic manner. The number of cells with apoptotic appearance described above increased with time prolonging after sodium nitroprusside treatment (Fig. 4a). The effect of sodium nitroprusside on disc cell apoptosis was further demonstrated by flow cytometry. As shown in Fig. 4b and c, there was no increase in apoptotic incidence of the monolayer-cultured annular cells within the first 1 h of sodium nitroprusside treatment. Starting from 2-h postsodium nitroprusside exposure, the apoptotic incidence increased significantly in a time-dependent manner when compared with the baseline.

Expression of biomarkers of ER stress and mitochondrial dysfunction in sodium nitroprusside-induced rat annular cell apoptosis

RT-PCR analysis indicated that there was the expression of GRP78 mRNA to some degree, but very little expression of GADD153 and caspase-12 mRNA at baseline in untreated rat annular cells. Treatment with 0.5 mM sodium nitroprusside significantly upregulated the mRNA expression of GRP78, GADD153, and caspase-12 in the annular cells, with GRP78 appearing first at 1-h postsodium nitroprusside treatment and GADD153 and caspase-12 occurring 2 h after the exposure (Fig. 5a, b). The expression of ER stress biomarkers was also examined at the protein level by immuofluorescence double labeling study. Very few apoptotic cells were visualized following Hoechst 33258 staining in untreated rat annular cells grown on glass coverslips. Under this baseline condition, there were a few GRP78- and GADD153-positive cells on the coverslips, but no caspase-12-positive cells were found. At the 3-h point after sodium nitroprusside treatment, the number of cells positive for GADD153 and GRP78 or GADD153 and caspase-12 increased dramatically along with the elevated numbers of the apoptotic cells. GRP78 and caspase-12 were localized in the cytoplasm and GADD153 in the nuclei of cells with brightly condensed or fragmented nuclei stained by Hoechst 33258. This phenomenon became more evident at the 6-h point after sodium nitroprusside treatment (Fig. 5c, d). Consistent with the RT-PCR and immuofluorescence staining findings, a weak band with a molecular weight of 78 kDa was noted in untreated rat disc annular cells, and this band became more and more intense at the 1-, 2-, 4-, and 6-h points after 0.5 mM sodium nitroprusside treatment. In the case of caspase-12, the band with a molecular weight of 50 kDa was barely detectable at baseline or at the 1-h point after sodium nitroprusside treatment, but the intensity of the caspase-12 band increased significantly over time starting 2 h postsodium nitroprusside treatment (Fig. 5e, f).

A time-dependent increase of cytochrome C accumulation in the cytosol of sodium nitroprusside-treated rat disc cells, as a protein band with a molecular weight of 11 kDa, was also detected at the 3- and 6-h points after sodium nitroprusside treatment (Fig. 5g, h).

Sodium nitroprusside treatment leads to decrease in mitochondrial membrane potential

To further document the involvement of mitochondrial dysfunction in the disc cell apoptosis, we measured mitochondrial membrane potential in the isolated rat annular cells with flow cytometry analysis and in situ JC-1 staining. As shown in Fig. 6a and b, the treatment with 0.5 mM sodium nitroprusside reduced mitochondrial membrane potential in a time-dependent manner, as indicated by a decrease in red/green ratio. The decrease in mitochondrial membrane potential, as monitored by in situ JC-1 staining, was seen primarily at the 3- and 6-h points after sodium nitroprusside treatment compared with the baseline (Fig. 6c).

Inhibition of sodium nitroprusside-induced apoptosis and caspase-9 activity by NS3694 and Z-ATAD-FMK

Either 100 μM NS3694 or 2 μM Z-ATAD-FMK significantly suppressed annular cell apoptosis induced by 0.5 mM sodium nitroprusside. Although apoptotic incidence further decreased after treatment with a combination of NS3694 and Z-ATAD-FMK, it did

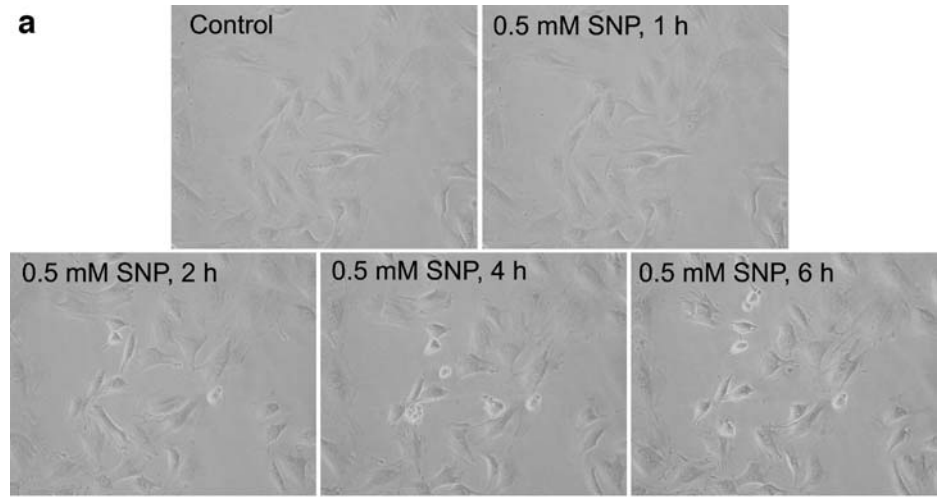
a
Control
0.5 mM SNP, 1 h
0.5 mM SNP, 2 h
0.5 mM SNP, 4 h
0.5 mM SNP, 6 h

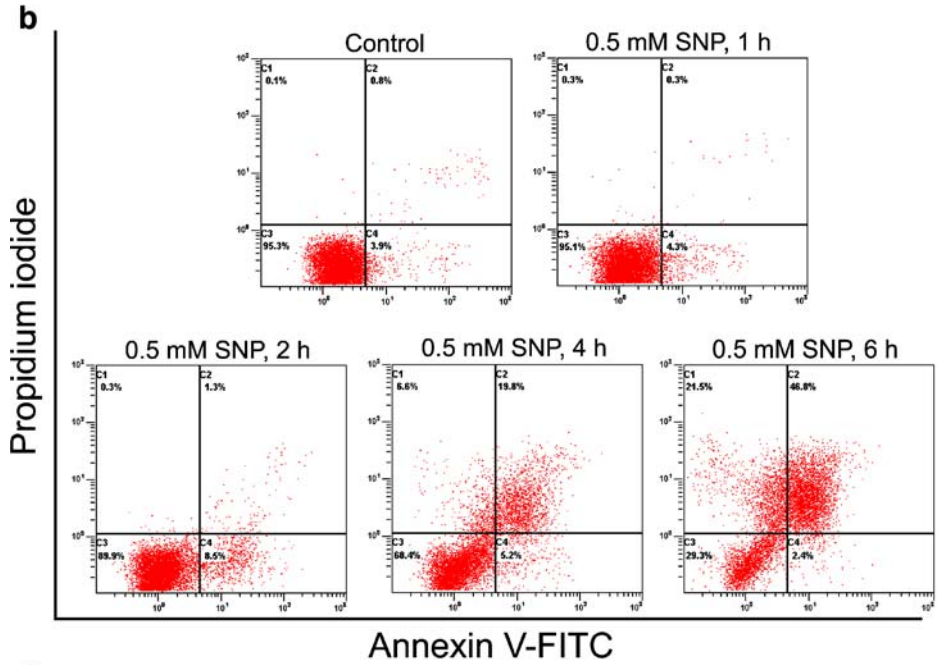
b
Control
0.5 mM SNP, 1 h
0.5 mM SNP, 2 h
0.5 mM SNP, 4 h
0.5 mM SNP, 6 h
Propidium iodide
Annexin V-FITC

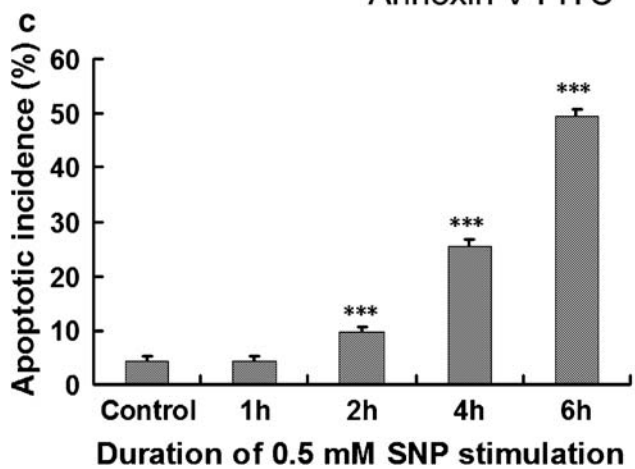
c
Apoptotic incidence (%)
60
50
40
30
20
10
0
***
***
***
Control
1h
2h
4h
6h
Duration of 0.5 mM SNP stimulation

◀ **Fig. 4** Sodium nitroprusside (SNP)-induced rat annular cell apoptosis detected by morphology and flow cytometry. **a** Dynamic morphologic changes during apoptosis of rat annular cells observed under an inverted phase-contrast microscopy (original magnification, ×320). **b** Typical pictures output by a flow cytometer. **c** Comparison of apoptotic incidence between groups. As compared with the control, ***$P<0.001$

not return to the level of negative controls (Fig. 7a, b). The suppression of sodium nitroprusside-induced apoptosis in rat disc cells was further documented by the measurement of caspase-9 activity. The exposure of the rat annular cells to 0.5 mM sodium nitroprusside for 6 h triggered a dramatic increase in caspase-9 activity as compared with vehicle controls. Similarly, either 100 μM NS3694 or 2 μM Z-ATAD-FMK significantly inhibited caspase-9 activity of annular cells treated by 0.5 mM sodium nitroprusside. Treatment with a combination of NS3694 and Z-ATAD-FMK further suppressed sodium nitroprusside-induced caspase-9 activation, but the caspase-9 activity did not decrease to the level of negative controls (Fig. 7c, d).

Discussion

Biomechanical disturbance plays a very important role in IVDD. As shown by epidemiological surveys (Battie et al. 1995; Stokes and Iatridis 2004), both overloading and immobilization of the spine contribute to IVDD. Various animal models also demonstrated that IVDD can be induced by different unphysiologic spinal loadings such as static axial compression (Lotz and Chin 2000; Lotz et al. 1998), static bending compression (Court et al. 2001), and dynamic axial compression (Walsh and Lotz 2004), associated with increased disc cell apoptosis.

In the current study, we employed unbalanced dynamic and static forces to induce rat lumbar IVDD, which is initially established by Wang et al. (2006a), and to induce rat cervical IVDD. With regard to why we used this modified method in the lumbar site, the reasons are as follows. First, the dorsal soft tissue in the cervical region is thicker than that in the lumbar region, thus increasing the surgical difficulty and death risk of the rats. Second, the lumbar vertebrae and discs are larger than the cervical ones, making it easy for imaging examination and harvest of disc tissues. Third, to reduce the experimental period, we further removed the spinous processes and posterolateral 1/2 of bilateral zygapophysial joints of the lumbar spine, which were reserved by Wang et al. (2006a) in their procedure for induction of rat cervical IVDD, to enhance the unbalanced dynamic and static forces of the lumbar spine.

With time prolonging after surgery, the degree of malalignment, disc space narrowing, and endplate calcification shown by lateral radiophotography of rat lumbar spine increased, the morphous of the annulus fibrosus shown by HE staining gradually revealed serpentine appearance with rupture, reversed contour, and indistinct, therefore confirming that IVDD was successfully induced. After surgery, disc cell apoptosis also increased over time, as shown by TUNEL staining. Spearman rank correlation test further revealed a significant positive relationship between the grade of IVDD and apoptotic incidence. These results strongly indicated that apoptosis is involved in rat lumbar IVDD induced by unbalanced dynamic and static forces.

The immunohistochemistry studies were to evaluate the expression of GRP78, GADD153, caspase-12, and the release of cytochrome C from the mitochondria by disc cells, as well as their relationships with apoptosis. In control group discs, there were a few GRP78- and GADD15-positive cells, indicating that a few disc cells would experience ER stress and growth arrest under normal condition. However, caspase-12- and cytochrome C-positive cells were seldom seen in these specimens, coincident with a very low TUNEL-positive incidence, indicating that apoptosis is scarce in normal rat discs. In the surgical group, GRP78-, GADD153-, caspase-12-, and cytochrome C-positive cells in the discs dramatically increased with time prolonging after surgery, illustrating that unbalanced dynamic and static forces of the spine significantly enhanced the expression of GRP78, GADD153, caspase-12, and the release of cytochrome C from the mitochondria. By Spearman rank correlation test, we found that disc cell apoptosis positively correlates with the expression of GRP78, GADD153, caspase-12, and the release of cytochrome C from the mitochondria, suggesting that mitochondria and ER were co-involved in disc cell apoptosis.

It is noteworthy that the numbers of GRP78- and GADD15-positive cells were much higher than that of caspase-12- and cytochrome C-positive cells. As

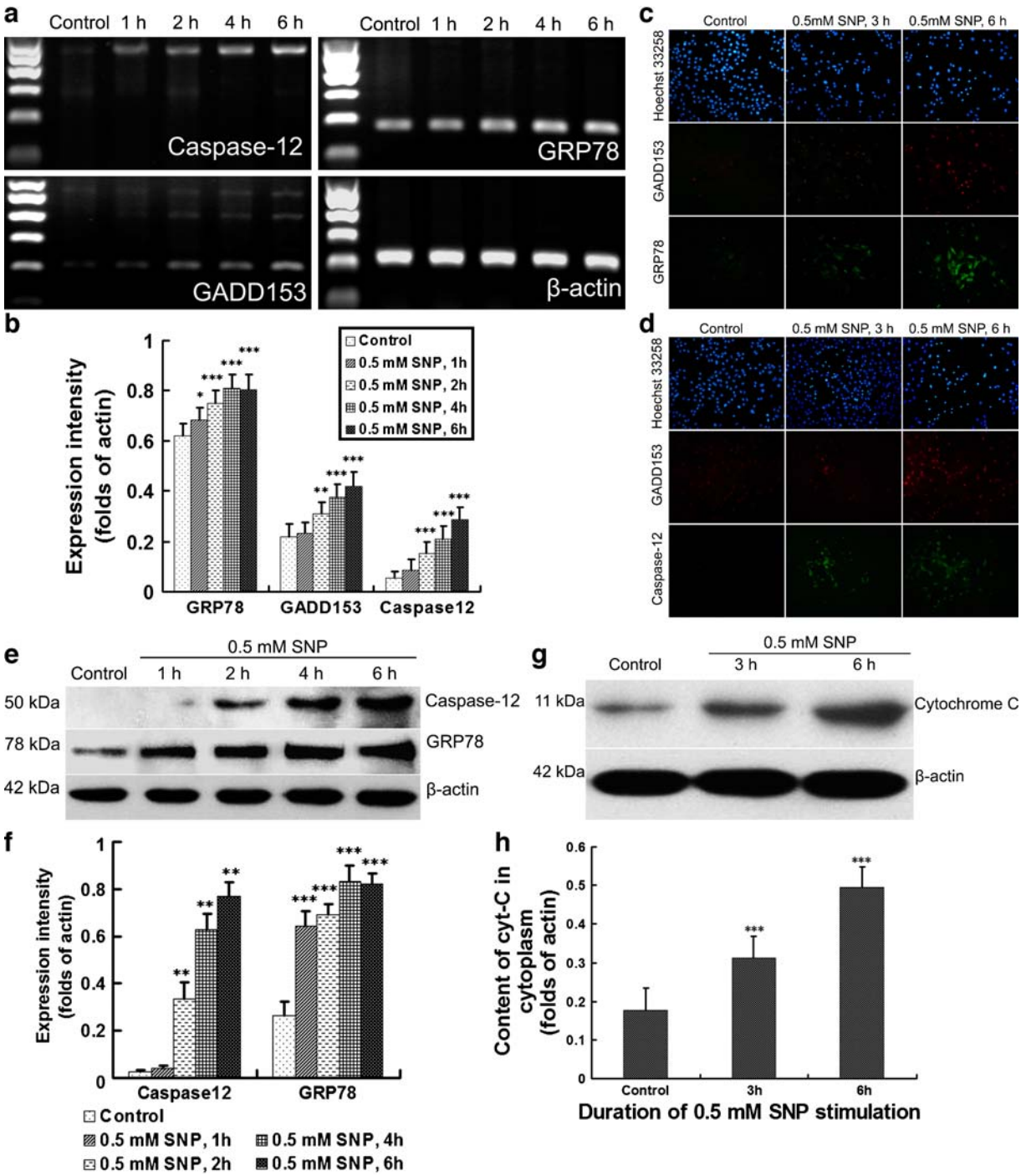

Fig. 5 Expression of biomarkers of ER stress and mitochondrial dysfunction in sodium nitroprusside (SNP)-induced rat annular cell apoptosis. **a** Typical photographs of gel electrophoresis of the PCR products. **b** Comparison of band intensity of GRP78, GADD153, and caspase-12 between groups. As compared with the control, *$P<0.05$, **$P<0.01$, ***$P<0.001$. **c**, **d** Fluorescence double labeling of GADD153 and GRP78, GADD153, and caspase-12. The three photographs in each column were taken under the same field. **e** Typical images of Western blot study. **f** Comparison of band intensity of GRP78 and caspase-12 between groups. As compared with the control, **$P<0.01$, ***$P<0.001$. **g** Typical images of Western blot study. **h** Comparison of band intensity of cytochrome C between groups. As compared with the control, ***$P<0.001$

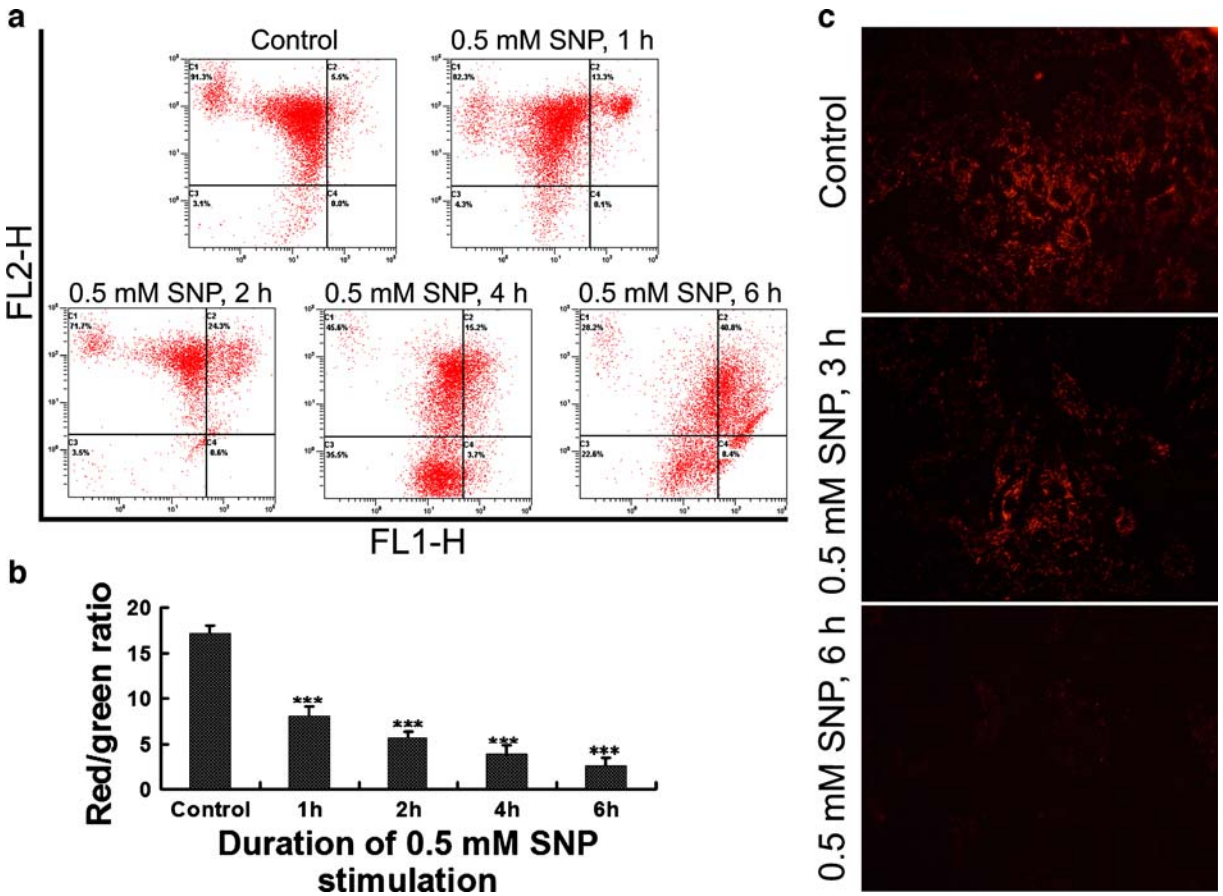

Fig. 6 Sodium nitroprusside (SNP) treatment leads to a decrease in mitochondrial membrane potential. **a** Typical pictures output by a flow cytometer. *Green* FL1-H, *red* FL2-H. **b** Comparison of mitochondrial membrane potential (red/green ratio) between groups. As compared with the control, ***$P<0.001$. **c** In situ JC-1 staining (original magnification, ×320). Decreased red fluorescence intensity indicating decreased amount of JC-1 polymer caused by decreased mitochondrial membrane potential

compared with apoptotic incidence, which was similar to that of caspase-12- and cytochrome C-positive cells, the incidences of GRP78- and GADD15-positive cells were also obviously higher. These results demonstrated that ER stress and growth arrest do not always lead to cell death, and apoptosis occurs only when caspase-12 is activated and cytochrome C is released from the mitochondria.

Although disc cells can be induced to apoptosis by serum deprivation via death receptor pathway (Park et al. 2006) and by cyclic stretch via mitochondria pathway (Rannou et al. 2004), stimuli which can lead to disc cell apoptosis via ER pathway has not been previously reported. The reasons for using sodium nitroprusside as apoptosis inducer in our in vitro experiments are as follows. First, super-physiological concentrations of nitric oxide not only results in DNA damage followed by depletion of the mitochondria (Wu et al. 2007) but also activate ER stress (Gotoh and Mori 2006), and apoptotic cell death occurs eventually. Second, there is evidence showing that sodium nitroprusside can induce apoptosis of cultured human disc cells (Kohyama et al. 2000). In the current study, the cultured rat annular cells sequentially exhibited shrink in size, plasma membrane blebbing, fragmentating into membrane-bound particles, and detachment of the whole cell after incubation with 0.5 mM sodium nitroprusside, confirming that sodium nitroprusside treatment led to cell death via apoptosis.

At the 1-h point after sodium nitroprusside treatment, the RT-PCR and Western blot analysis

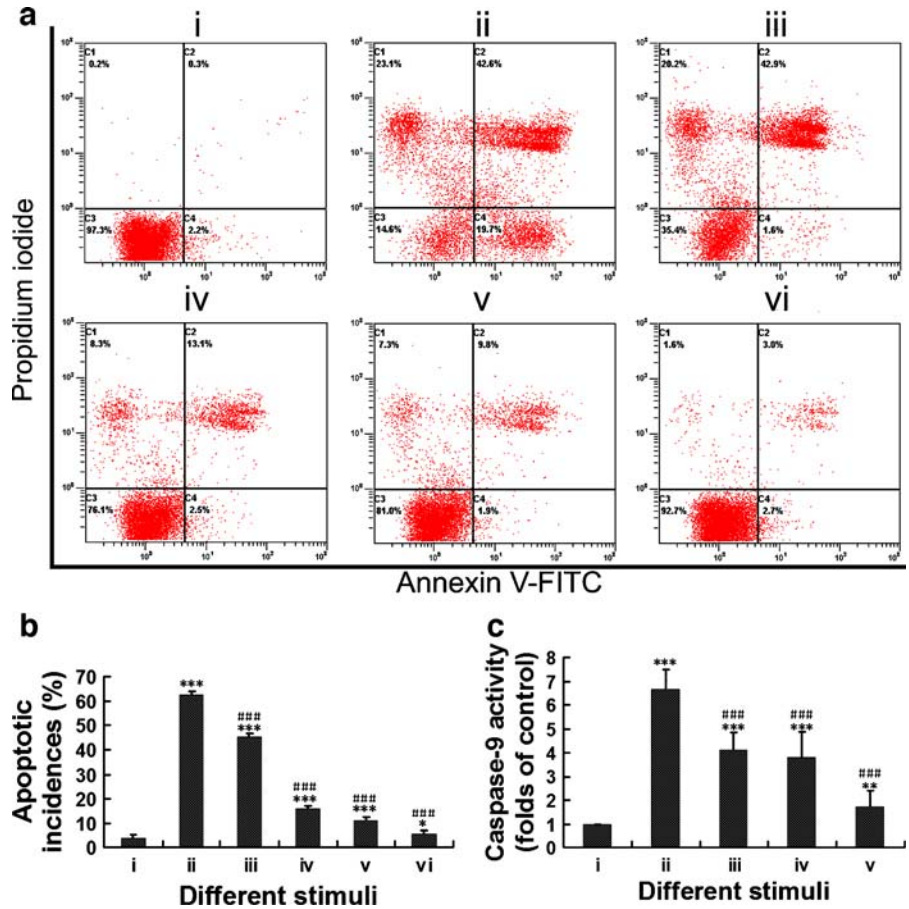

Fig. 7 Inhibition of sodium nitroprusside-induced apoptosis and caspase-9 activity by NS3694 and Z-ATAD-FMK. **a** Typical pictures output by a flow cytometer. **b** Comparison of apoptotic incidence between groups. As compared with group *i*, $*P<0.05$, $***P<0.001$. As compared with group *iii*, $^{###}P<0.001$. *i* Negative control, *ii* 1 μM thapsigargin for 6 h, served as positive control, *iii* 0.5 mM sodium nitroprusside for 6 h, *iv* 100 μM NS3694 for 1 h followed by 0.5 mM sodium nitroprusside for 6 h, *v* 2 μM Z-ATAD-FMK for 1 h followed by 0.5 mM sodium nitroprusside for 6 h, *vi* 100 μM NS3694 plus 2 μM Z-ATAD-FMK for 1 h followed by 0.5 mM sodium nitroprusside for 6 h. **c** The effects of NS3694 and Z-ATAD-FMK on caspase-9 activity. As compared with group *i*, $**P<0.001$, $***P<0.001$. As compared with group *ii*, $^{###}P<0.001$. *i* Negative control, *ii* 0.5 mM sodium nitroprusside for 6 h; *iii* 100 μM NS3694 for 1 h followed by 0.5 mM sodium nitroprusside for 6 h, *iv* 2 μM Z-ATAD-FMK for 1 h followed by 0.5 mM sodium nitroprusside for 6 h, *v* 100 μM NS3694 plus 2 μM Z-ATAD-FMK for 1 h followed by 0.5 mM sodium nitroprusside for 6 h

showed that the expression of GRP78 increased, whereas the expression of GADD153 and caspase-12 did not change, and flow cytometry did not show an increase in apoptotic incidence. These results indicated that sodium nitroprusside treatment led to ER stress at first. From the 2-h point after sodium nitroprusside treatment, the expression of GADD153 and caspase-12 upregulated while apoptotic incidence increased, suggesting that the cells failed to resist the prolonged ER stress and eventually went into apoptosis via the ER pathway. This was further supported by the fluorescence double labeling studies, which demonstrated that GRP78, GADD153, and caspase-12 were increasingly expressed by the cells that underwent apoptosis, as confirmed by Hoechst 33258 staining.

The mitochondria pathway is another important pathway in apoptotic process (Orrenius 2004). When cell damage is unrepairable, a decrease in the mitochondrial membrane potential and the release of cytochrome C into the cytoplasm may occur. Once cytochrome C is released, it binds to apoptotic

protease activating factor-1, triggering formation of the apoptosome, which in turn activates caspase-9 and leads to apoptosis. Our results also revealed a decrease in the mitochondrial membrane potential and an increase in the amount of cytochrome C in the cytoplasm after sodium nitroprusside treatment, suggesting that the mitochondrial pathway was also involved in sodium nitroprusside-induced disc cell apoptosis. Interestingly, an evident decrease in mitochondrial membrane potential was observed even at the 1-h point after sodium nitroprusside treatment, but the apoptotic incidence did not increase at the same time. This might be explained by the fact that decreased mitochondrial membrane potential do not always lead to apoptosis (Lopez-Armada et al. 2006); it also indicated that the decrease in mitochondrial membrane potential was an upstream event but not the result of disc cell apoptosis.

There is evidence showing that some cytokines such as platelet-derived growth factor and insulin-like growth factor 1 can inhibit disc cell apoptosis in vitro (Gruber et al. 2000; Wang et al. 2006b); the underlying signal transduction pathways, however, have not been elucidated. In addition, although previous studies about disc cell apoptosis considered the activation of caspase-9 as the specific marker of the involvement of mitochondrial pathway (Park et al. 2005, 2006; Rannou et al. 2004), there is also evidence suggesting that caspase-9 can be activated by caspase-12 independent of cytochrome C release from the mitochondria (Morishima et al. 2002), indicating that the activation of caspase-9 is a common target downstream to mitochondria and ER dysfunction. In our opinion, release of cytochrome C from the mitochondria and formation of the apoptosome complex indicates the involvement of mitochondrial pathway in the process of apoptosis, and the activation of caspase-12 indicates the involvement of ER pathway.

To verify whether ER and mitochondria were co-involved in sodium nitroprusside-induced rat annular cell apoptosis, we employed NS3694 to inhibit the formation of the apoptosome and employed Z-ATAD-FMK to suppress the activation of caspase-12. Our results showed that either NS3694 or Z-ATAD-FMK significantly suppressed caspase-9 activation and apoptosis of rat annular cell induced by sodium nitroprusside, and these effects were further enhanced by the combination of NS3694 and Z-ATAD-FMK, also suggesting the co-involvement of ER and mitochondria in rat annular cell apoptosis.

The current study is the first to demonstrate that disc cells can undergo apoptosis *via* ER pathway both in vivo and in vitro. It has long been recognized that IVDD is, to a considerable extent, a process of destruction and failure of the extracellular matrix, which is produced and maintained by disc cells and that apoptosis plays an important role in cellular loss in the disc. Thus, suppression of ER-mediated apoptosis may prevent the decrease in disc cell population and therefore be a potential strategy for retarding IVDD.

In addition, although disc cell apoptosis via mitochondria pathway or death receptor pathway has been demonstrated previously, studies focused on the extensive relationships among various signal transduction pathways are very few. To date, only the cross-talk between mitochondria pathway and death receptor pathway in the process of disc cell apoptosis has been demonstrated (Park et al. 2005). Thus, the current study aimed to investigate whether the familiar pathway, mitochondria pathway, and a relatively new pathway, which has not been reported in this research field, ER pathway, are co-involved in disc cell apoptosis and IVDD. Our results also suggest that the signal transduction pathways of disc apoptosis are more complex than our expectation.

Acknowledgments This study was supported by the National Natural Science Foundation of China (no. 30700851) and Science and Technology Commission of Shanghai Municipality (09411953000).

Disclosures All authors have nothing to declare.

References

Adams JM (2003) Ways of dying: multiple pathways to apoptosis. Genes Dev 17:2481–2495

Ariga K, Miyamoto S, Nakase T, Okuda S, Meng W, Yonenobu K et al (2001) The relationship between apoptosis of endplate chondrocytes and aging and degeneration of the intervertebral disc. Spine 26:2414–2420

Ariga K, Yonenobu K, Nakase T, Hosono N, Okuda S, Meng W et al (2003) Mechanical stress-induced apoptosis of endplate chondrocytes in organ-cultured mouse intervertebral discs: an ex vivo study. Spine 28:1528–1533

Battie MC, Videman T, Gibbons LE, Fisher LD, Manninen H, Gill K (1995) Determinants of lumbar disc degeneration: a study relating lifetime exposures and magnetic resonance imaging findings in identical twins. Spine 20:2601–2612

Benavides A, Pastor D, Santos P, Tranque P, Calvo S (2005) CHOP plays a pivotal role in the astrocyte death induced by oxygen and glucose deprivation. Glia 52:261–275

Court C, Colliou OK, Chin JR, Liebenberg E, Bradford DS, Lotz JC (2001) The effect of static in vivo bending on the murine intervertebral disc. Spine J 1:239–245

Ferreiro E, Costa R, Marques S, Cardoso SM, Oliveira CR, Pereira CM (2008) Involvement of mitochondria in endoplasmic reticulum stress-induced apoptotic cell death pathway triggered by the prion peptide PrP(106–126). J Neurochem 104:766–776

Fernandez-Segura E, Canizares FJ, Cubero MA, Warley A, Campos A (1999) Changes in elemental content during apoptotic cell death studied by electron probe X-ray microanalysis. Exp Cell Res 253:454–462

Gotoh T, Mori M (2006) Nitric oxide and endoplasmic reticulum stress. Arterioscler Thromb Vasc Biol 26:1439–1446

Gruber HE, Hanley EN Jr (1998) Analysis of aging and degeneration of the human intervertebral disc. Comparison of surgical specimens with normal controls. Spine 23:751–757

Gruber HE, Norton HJ, Hanley EN Jr (2000) Anti-apoptotic effects of IGF-1 and PDGF on human intervertebral disc cells in vitro. Spine 25:2153–2157

Groenendyk J, Michalak M (2005) Endoplasmic reticulum quality control and apoptosis. Acta Biochim Pol 52:381–395

Kadowaki H, Nishitoh H, Ichijo H (2004) Survival and apoptosis signals in ER stress: the role of protein kinases. J Chem Neuroanat 28:93–100

Kohyama K, Saura R, Doita M, Mizuno K (2000) Intervertebral disc cell apoptosis by nitric oxide: biological understanding of intervertebral disc degeneration. Kobe J Med Sci 46:283–295

Kroeber MW, Unglaub F, Wang H, Schmid C, Thomsen M, Nerlich A et al (2002) New in vivo animal model to create intervertebral disc degeneration and to investigate the effects of therapeutic strategies to stimulate disc regeneration. Spine 27:2684–2690

Lademann U, Cain K, Gyrd-Hansen M, Brown D, Peters D, Jaattela M (2003) Diarylurea compounds inhibit caspase activation by preventing the formation of the active 700-kilodalton apoptosome complex. Mol Cell Biol 23:7829–7837

Liu N, Kuang X, Kim HT, Stoica G, Qiang W, Scofield VL et al (2004) Possible involvement of both endoplasmic reticulum- and mitochondria-dependent pathways in MoMuLV-ts1-induced apoptosis in astrocytes. J Neurovirol 10:189–198

Lopez-Armada MJ, Carames B, Martin MA, Cillero-Pastor B, Lires-Dean M, Fuentes-Boquete I et al (2006) Mitochondrial activity is modulated by TNF-α and IL-1β in normal human chondrocyte cells. Osteoarthritis Cartilage 14:1011–1022

Lotz JC, Chin JR (2000) Intervertebral disc cell death is dependent on the magnitude and duration of spinal loading. Spine 25:1477–1483

Lotz JC, Colliou OK, Chin JR, Duncan NA, Liebenberg E (1998) Compression-induced degeneration of the intervertebral disc: an in vivo mouse model and finite-element study. Spine 23:2493–2506

Luo S, Mao C, Lee B, Lee AS (2006) GRP78/BiP is required for cell proliferation and protecting the inner cell mass from apoptosis during early mouse embryonic development. Mol Cell Biol 26:5688–5697

Luthra S, Dong J, Gramajo AL, Chwa M, Kim DW, Neekhra A et al (2008) 7-Ketocholesterol activates caspases-3/7, -8, and -12 in human microvascular endothelial cells in vitro. Microvasc Res 75:343–350

Nishimura K, Mochida J (1998) Percutaneous reinsertion of the nucleus pulposus. An experimental study. Spine 23:1531–1539

Masud A, Mohapatra A, Lakhani SA, Ferrandino A, Hakem R, Flavell RA (2007) Endoplasmic reticulum stress-induced death of mouse embryonic fibroblasts requires the intrinsic pathway of apoptosis. J Biol Chem 282:14132–14139

McCullough KD, Martindale JL, Klotz LO, Aw TY, Holbrook NJ (2001) Gadd153 sensitizes cells to endoplasmic reticulum stress by down-regulating Bcl2 and perturbing the cellular redox state. Mol Cell Biol 21:1249–1259

Morishima N, Nakanishi K, Takenouchi H, Shibata T, Yasuhiko Y (2002) An endoplasmic reticulum stress-specific caspase cascade in apoptosis: cytochrome c-independent activation of caspase-9 by caspase-12. J Biol Chem 277:34287–34294

Mulhern ML, Madson CJ, Danford A, Ikesugi K, Kador PF, Shinohara T (2006) The unfolded protein response in lens epithelial cells from galactosemic rat lenses. Invest Ophthalmol Vis Sci 47:3951–3959

Nagata T, Ilieva H, Murakami T, Shiote M, Narai H, Ohta Y et al (2007) Increased ER stress during motor neuron degeneration in a transgenic mouse model of amyotrophic lateral sclerosis. Neurol Res 29:767–771

Oliver BL, Cronin CG, Zhang-Benoit Y, Goldring MB, Tanzer ML (2005) Divergent stress responses to IL-1β, nitric oxide, and tunicamycin by chondrocytes. J Cell Physiol 204:45–50

Orrenius S (2004) Mitochondrial regulation of apoptotic cell death. Toxicol Lett 149:19–23

Park JB, Chang H, Kim KW (2001a) Expression of Fas ligand and apoptosis of disc cells in herniated lumbar disc tissue. Spine 26:618–621

Park JB, Kim KW, Han CW, Chang H (2001b) Expression of Fas receptor on disc cells in herniated lumbar disc tissue. Spine 26:142–146

Park JB, Lee JK, Park SJ, Kim KW, Riew KD (2005) Mitochondrial involvement in fas-mediated apoptosis of human lumbar disc cells. J Bone Joint Surg Am 87:1338–1342

Park JB, Park IC, Park SJ, Jin HO, Lee JK, Riew KD (2006) Anti-apoptotic effects of caspase inhibitors on rat intervertebral disc cells. J Bone Joint Surg Am 88:771–779

Rannou F, Lee TS, Zhou RH, Chin J, Lotz JC, Mayoux-Benhamou MA et al (2004) Intervertebral disc degeneration:

the role of the mitochondrial pathway in annulus fibrosus cell apoptosis induced by overload. Am J Pathol 164:915–924

Reddy RK, Mao C, Baumeister P, Austin RC, Kaufman RJ, Lee AS (2003) Endoplasmic reticulum chaperone protein GRP78 protects cells from apoptosis induced by topoisomerase inhibitors: role of ATP binding site in suppression of caspase-7 activation. J Biol Chem 278:20915–20924

Sanges D, Marigo V (2006) Cross-talk between two apoptotic pathways activated by endoplasmic reticulum stress: differential contribution of caspase-12 and AIF. Apoptosis 11:1629–1641

Stokes IA, Iatridis JC (2004) Mechanical conditions that accelerate intervertebral disc degeneration: overload versus immobilization. Spine 29:2724–2732

Tan Y, Dourdin N, Wu C, De Veyra T, Elce JS, Greer PA (2006) Ubiquitous calpains promote caspase-12 and JNK activation during endoplasmic reticulum stress-induced apoptosis. J Biol Chem 281:16016–16024

Unterberger U, Hoftberger R, Gelpi E, Flicker H, Budka H, Voigtlander T (2006) Endoplasmic reticulum stress features are prominent in Alzheimer disease but not in prion diseases in vivo. J Neuropathol Exp Neurol 65:348–357

Walsh AJ, Lotz JC (2004) Biological response of the intervertebral disc to dynamic loading. J Biomech 37:329–337

Wang YJ, Shi Q, Lu WW, Cheung KC, Darowish M, Li TF et al (2006a) Cervical intervertebral disc degeneration induced by unbalanced dynamic and static forces: a novel in vivo rat model. Spine 31:1532–1538

Wang YJ, Shi Q, Sun P, Zhou Q, Darowish M, Li TF et al (2006b) Insulin-like growth factor-1 treatment prevents anti-Fas antibody-induced apoptosis in endplate chondrocytes. Spine 31:736–741

Williams BL, Lipkin WI (2006) Endoplasmic reticulum stress and neurodegeneration in rats neonatally infected with borna disease virus. J Virol 80:8613–8626

Wu GJ, Chen TG, Chang HC, Chiu WT, Chang CC, Chen RM (2007) Nitric oxide from both exogenous and endogenous sources activates mitochondria-dependent events and induces insults to human chondrocytes. J Cell Biochem 101:1520–1531

Xu H, Zhou Q, Liu X, Qi YP (2006) Co-involvement of the mitochondria and endoplasmic reticulum in cell death induced by the novel ER-targeted protein HAP. Cell Mol Biol Lett 11:249–255

Zhao CQ, Jiang LS, Dai LY (2006) Programmed cell death in intervertebral disc degeneration. Apoptosis 11:2079–2088

Zhao CQ, Liu D, Li H, Jiang LS, Dai LY (2007) Interleukin-1β enhances the effect of serum deprivation on rat annular cell apoptosis. Apoptosis 12:2155–2161

Yang L, Carlson SG, McBurney D, Horton WE Jr (2005) Multiple signals induce endoplasmic reticulum stress in both primary and immortalized chondrocytes resulting in loss of differentiation, impaired cell growth, and apoptosis. J Biol Chem 280:31156–31165